

Semi-constraint Optimal Transport for Entity Alignment with Dangling Cases

Shengxuan Luo¹ Pengyu Cheng² Sheng Yu¹

¹Tsinghua University ²Duke University

luosx18@mails.tsinghua.edu.cn

Abstract

Entity alignment (EA) merges knowledge graphs (KGs) by identifying the equivalent entities in different graphs, which can effectively enrich knowledge representations of KGs. However, in practice, different KGs often include *dangling entities* whose counterparts cannot be found in the other graph, which limits the performance of EA methods. To improve EA with dangling entities, we propose an unsupervised method called **Semi-constraint Optimal Transport for Entity Alignment in Dangling cases (SoTead)**. Our main idea is to model the entity alignment between two KGs as an optimal transport problem from one KG’s entities to the others. First, we set pseudo entity pairs between KGs based on pretrained word embeddings. Then, we conduct contrastive metric learning to obtain the transport cost between each entity pair. Finally, we introduce a *virtual entity* for each KG to “align” the dangling entities from the other KGs, which relaxes the optimization constraints and leads to a semi-constraint optimal transport. In the experimental part, we first show the superiority of SoTead on a commonly-used entity alignment dataset. Besides, to analyze the ability for dangling entity detection with other baselines, we construct a medical cross-lingual knowledge graph dataset, MedED, where our SoTead also reaches state-of-the-art performance.

1 Introduction

Knowledge graphs (KGs) has become one of the essential modules in various intelligent domains, such as question-answering (Savenkov and Agichtein, 2016; Yu et al., 2017; Jin et al., 2021), recommendation (Cao et al., 2019), and search engines (Xiong et al., 2017). However, constructing a large-scale KG consumes massive computational resources (Paulheim, 2018) and can be easily trapped into knowledge incompleteness (Galárraga et al., 2017). Therefore, under real-world scenarios, merging multiple KGs by entity alignment (EA) becomes a

mainstream solution to enrich knowledge of KGs. More specifically, entity alignment combines different KGs by aligning the equivalent entities across the KGs (Zhang et al., 2020; Zeng et al., 2021a).

To detect the identical entities, prior works of entity alignment mainly focus on embedding-level alignment by learning a representation vector for each entity, so that the similar entities can locate closely to each others in the embedding spaces (Chen et al., 2017; Sun et al., 2018; Wang et al., 2018; Zhu et al., 2021a; Liu et al., 2021; Lin et al., 2021). These embedding-based EA methods always require an impractical assumption, that for each entity there always exists a counterpart in the other KG (Sun et al., 2021). Moreover, the embedding-level EA methods evaluate their performances only on the existing entity pairs between the testing KGs. However, in various real-world scenarios, the identical pair of one entity is not guaranteed to exist between different KGs (Zhao, 2020; Sun et al., 2021), which limits the application range of embedding-based EA methods.

Recently, the aforementioned unmatchable entities in KGs have been recognized as the *dangling entities* (Sun et al., 2021). To improve the EA performance, it is necessary to identify the dangling entities and then align the remaining matchable entities to their counterparts. Hence, a limited number of prior works attempt to address the dangling entities detection (DED). Zhao et al. (2020) and Zeng et al. (2021b) apply thresholds on the embedding distance of each entity and its nearest neighbor to determine if the entity is dangling. Nevertheless, the threshold cuts are not flexible enough when considering the relative entity distances. For example, a dangling entity could have an available distance (smaller than the threshold) to a target entity, while the target one has even closer distance to the ground-truth counterpart.

Sun et al. (2021) constructs a labeled training set of dangling entities and trains a neural classifier to

predict whether each entity is matchable. However, this supervised method has limited practicability for the difficulty of creating training sets in real-world large-scale KGs.

To solve the dangling entities within an unsupervised scheme and a global perspective, we propose **SoTead**, a **Semi-constraint Optimal Transport** method for **Entity Alignment with Dangling** cases. ((Instead of matching the entities with their closest neighbors)), we consider a global optimal entity matching by solving the optimal transport between the groups of entities in two KGs. Our unsupervised method consists of two parts: (1) estimating the cross-KG entity similarity with the textual information of entity names and a contrastive distance learning in entity embedding space; (2) solving a *semi-constraint* optimal transport (OT) between two KG entity sets to discover the globally optimal entity matching based on the estimated entity similarities. Since the dangling entities cannot “transport” to the target KG, we introduce a virtual entity in the target KG and relax the OT constraints, so that the dangling entities can be matched to the virtual entity instead. On the other hand, the virtual entity also works as a dangling entities detector in the solution of our semi-constraint OT optimization, for only dangling entities in the target KG with match to it. To empirically demonstrate the effectiveness of our SoTead method, we conduct the experiments on both the entity alignment (EA) and dangling entity detection (DED) tasks. Since there is no testing set for dangling entity detection, we also construct a cross-lingual medical knowledge graph dataset, MedED. Our experiments show that the dangling entity identification mechanism also enhances the EA performance. On both of the EA and DED tasks, our method achieves remarkable performance improvement even comparing with baselines under supervised setups.

The main contributions of this paper is summarized in follows:

- We propose SoTead, an unsupervised entity alignment method via semi-constraint optimal transport, which can jointly match paired entities and detect unmatchable entities.
- To demonstrate the effectiveness of our model, we create a cross-lingual knowledge graph dataset, MedED, which supports the evaluation for both entity alignment and dangling entity detection.
- We achieve state-of-the-art performance on

comprehensive experiments of entity alignment and dangling entity detection, and analyze the impacts of high-quality dangling entity detection for improving entity alignment.

The source code is publicly available at <https://github.com/luosx18/UED>.

2 Preliminary

Optimal Transport: Optimal Transport (OT) aims to find the minimal cost for transporting the density distribution of group of items to that of another group, given all the unit transportation cost between each item pairs (Villani, 2009). In formula, OT between density $p \in \mathbb{R}^n$ and $q \in \mathbb{R}^m$ is:

$$D_C(p, q) := \min_{\mathbf{X}} \langle \mathbf{C}, \mathbf{X} \rangle, \quad (1)$$

$$\text{s.t. } \mathbf{X}^T \mathbf{1}_m = \mathbf{p}, \mathbf{X} \mathbf{1}_n = \mathbf{q},$$

$$\mathbf{q}^T \mathbf{1}_n = \mathbf{p}^T \mathbf{1}_m,$$

where $\langle \mathbf{C}, \mathbf{X} \rangle = \sum_{i=1}^n \sum_{j=1}^m c_{ij} x_{ij}$ is the matrix inner product between cost matrix $\mathbf{C} = [c_{ij}]_{m \times n}$ and the transited density $\mathbf{X} = [x_{ij}]_{m \times n}$, and $\mathbf{1}_m, \mathbf{1}_n$ are all-one vectors.

Since the OT objective is symmetric for both density q and p , OT has been recognized as an effective match approach and shown noticeable matching performance in many machine leaning tasks. For example, in machine translation, Alvarez-Melis and Jaakkola (2018) uses OT to measure the similarity of generated translation with ground-truth, by matching sentences as two groups of words. Besides, OT has shown improvements on other natural language processing tasks, such as document retrieval (Kusner et al., 2015), text generation (Salimans et al., 2018; Chen et al., 2018), and sequence-to-sequence learning (Chen et al., 2019).

Mixed Integer Programming: Linear programming (LP) is a fundamental method to optimize linear objective functions with linear constraints (Padberg and Rinaldi, 1991; Gass, 2003; Dantzig, 2016). Mathematically, LP is formed as:

$$\min \mathbf{c}^T \mathbf{x}, \quad (2)$$

$$\text{s.t. } \mathbf{A} \mathbf{x} \leq \mathbf{b},$$

$$\mathbf{x} \geq \mathbf{0},$$

where $\mathbf{x} = (x_1, x_2, \dots, x_n)^T$ is the vector of n variables, $\mathbf{A} \mathbf{x} \leq \mathbf{b}$ ($\mathbf{A} \in \mathbb{R}^{m \times n}, \mathbf{b} \in \mathbb{R}^m$) are m linear constrains, and $\mathbf{c}^T \mathbf{x}$ is the linear objective. When considering the linear programming with continuous variables, the simplex algorithm

is widely-used, which efficiently searches the optimal solution on the vertices of the feasible region (Dantzig et al., 1955). However, when limiting some of the variables to be integers, the linear programming becomes more challenging, leading to the problem of mixed integer programming (MIP).

A common solution to MIP is the branch-and-cut algorithm (Wolsey and Nemhauser, 1999; Mitchell, 2002), which first solves the relaxed linear programming without the integer constraints via the simplex method, and then iteratively branches the MIP by splitting the constraint space based on one of the non-integer variables. For every branch, a relaxed linear programming is solved to check if the relaxation is infeasible. If the relaxation is infeasible or less optimal than current solution, the corresponding branch will be pruned. Otherwise, the branch process will continue until all the constraints are satisfied (details in the Supplementary A.1). Besides, Balas et al. (1993); Mitchell (2002) accelerate the solving of the MIP via a cutting plane algorithm for constraint branching.

3 Proposed Method

In this section, we first jointly model the entity alignment and dangling entity detection within a semi-constraint optimal transport framework. Then we describe how to obtain the entity distances across the KGs under an unsupervised setup. At last, we analyze the numerical solution and efficiency of the semi-constraint optimal transport.

3.1 Semi-constraint Optimal Transport

We define a knowledge graph as $\mathcal{G} = \{\mathcal{E}, \mathcal{R}\}$, where \mathcal{E} is the entity set, and \mathcal{R} denotes the set of entity relations. Furthermore, we consider the entity set $\mathcal{E} = \mathcal{D} \cup \mathcal{A}$ as a disjoint union of the dangling set \mathcal{D} and matchable set \mathcal{A} . For two KGs, $\mathcal{G}_1 = \{\mathcal{D}_1 \cup \mathcal{A}_1, \mathcal{R}_1\}$ and $\mathcal{G}_2 = \{\mathcal{D}_2 \cup \mathcal{A}_2, \mathcal{R}_2\}$, our task is to align the matchable entities in \mathcal{A}_1 and \mathcal{A}_2 and detect the dangling set \mathcal{D}_1 and \mathcal{D}_2 jointly.

Denote entities in \mathcal{G}_1 as $\mathcal{E}_1 = \{u_1, u_2, \dots, u_m\}$ and entities in \mathcal{G}_2 as $\mathcal{E}_2 = \{v_1, v_2, \dots, v_n\}$. Then entity alignment is to find equivalent pairs $\{(u_i, v_j) | u_i \in \mathcal{A}_1, v_j \in \mathcal{A}_2\}$. As in Section 2, we convert this matching problem to an optimal transport from \mathcal{E}_1 to \mathcal{E}_2 by minimizing the dissimilarity scores $\{d(u_i, v_j)\}$ as the transportation cost. Hence, we introduce indicators:

$$\psi_{ij} = \begin{cases} 1, & \text{if } u_i \text{ matches } v_j \\ 0, & \text{if } u_i \text{ does not match } v_j \end{cases} \quad (3)$$

With the indicators ψ_{ij} , we convert the global entity alignment in to the following objective:

$$\begin{aligned} \min & \sum_{i=1}^m \sum_{j=1}^n c_{ij} \psi_{ij}, \\ \text{s.t.} & \sum_{j=1}^n \psi_{ij} = 1, \quad 1 \leq i \leq m, \\ & \sum_{i=1}^m \psi_{ij} = 1, \quad 1 \leq j \leq n, \end{aligned} \quad (4)$$

where the cost $c_{ij} = d(u_i, v_j) > 0$ is set to the dissimilarity between entity pair (u_i, v_j) . The summation constraints indicate each entity in \mathcal{E}_1 can only match to one entity in \mathcal{E}_2 and vice versa.

However, when \mathcal{E}_1 and \mathcal{E}_2 have different numbers of entities ($n \neq m$), the constraints in equation (4) can never be satisfied. Besides, the dangling entities are not considered in the above optimal transport. To address these issues, we introduce ‘‘virtual’’ entities u_0 and v_0 into \mathcal{E}_1 and \mathcal{E}_2 respectively. With the two virtual entities u_0 and v_0 , we can further relax the constraints of indicators:

$$\begin{aligned} \min & \sum_{i=1}^m \sum_{j=1}^n c_{ij} \psi_{ij} + \sum_{i=1}^m c_{i,0} \psi_{i,0} + \sum_{j=1}^n c_{0,j} \psi_{0,j} \\ \text{s.t.} & \sum_{j=1}^n \psi_{ij} = 1, \quad 1 \leq i \leq m, \\ & \sum_{i=1}^m \psi_{ij} = 1, \quad 1 \leq j \leq n. \end{aligned} \quad (5)$$

Since no marginal constraint is added to $\{\psi_{0,j}\}_{j=1}^n$ and $\{\psi_{i,0}\}_{i=1}^m$, arbitrary number of dangling entities can be aligned to u_0 and v_0 , which means the constraints in equation (5) are always feasible. Note that we do not consider the distance $c_{0,0} = d(u_0, v_0)$ between the two virtual entities, because the alignment $\psi_{0,0}$ between u_0 and v_0 is meaningless and can lead to the degeneration of the optimization.

Also, the distances between virtual entities and real entities have not been defined. Here, we introduce two hyper-parameters $\alpha, \beta > 0$, as the cross KG distances between the virtual entities and real entities, $c_{0,j} = \alpha, c_{i,0} = \beta$ ($1 \leq j \leq n$ and $1 \leq i \leq m$). The details about the selection of α and β are described in Section 3.2. Therefore, the final optimization of our semi-constraint optimal transport is in equation (6). By solving equation (6), we jointly obtain the solutions for entity

alignment (with $\{\psi_{ij}\}_{1 \leq i \leq m, 1 \leq j \leq n}$) and dangling entity detection (with $\{\psi_{0,j}\}_{j=1}^n$ and $\{\psi_{i,0}\}_{i=1}^m$). In the followings, we first describe how we obtain the entity distances c_{ij} in Section 3.2, then discuss how to solve the semi-constraint optimal transport in Section 3.3.

$$\begin{aligned} \min & \sum_{i=1}^m \sum_{j=1}^n c_{ij} \psi_{ij} + \beta \sum_{i=1}^m \psi_{i,0} + \alpha \sum_{j=1}^n \psi_{0,j} \\ \text{s.t.} & \sum_{j=1}^n \psi_{ij} = 1, \quad 1 \leq i \leq m, \\ & \sum_{i=1}^m \psi_{ij} = 1, \quad 1 \leq j \leq n. \end{aligned} \quad (6)$$

3.2 Entity Distance Learning

As shown in Figure 1, our unsupervised entity distance learning scheme consists of three steps: (1) set a group of pseudo entity pairs based on the textual information of entity names; (2) with the guidance of pseudo pairs, conduct a contrastive embedding learning on entity sample pairs; (3) utilize the textual embedding of all entities to build a globally guided refining loss. The details of the three steps is described below.

Pseudo entity pairs: We utilize GloVe (Pennington et al., 2014) word embeddings to obtain entity name textual embeddings w_i^u, w_j^v for entities $u_i \in \mathcal{E}_1$ and $v_j \in \mathcal{E}_2$ respectively. Then the initial similarity is defined as $s_{ij} = \cos(w_i^u, w_j^v)$. By setting a threshold $0 < \varepsilon < 1$, we select pseudo entity pairs when s_{ij} satisfies: (a) $s_{ij} > \varepsilon$; (b) $s_{ik} \leq \varepsilon$, for any $k \neq j$; (c) $s_{lj} \leq \varepsilon$, for any $l \neq i$. We denote the pseudo entity pairs set as \mathcal{P} . For cross-lingual KGs, we translate entity names via machine translation before extracting textual information.

Contrastive alignment loss: We use the Pseudo entity pair to induce the learning of enhanced entity embeddings e_i^u and e_j^v for u_i and v_j respectively. Each entity embedding is encoded with a graph neural network (GNN), which takes the textual embedding as node embedding and KG relations as the graph edges. For each pseudo pair $(u_i, v_j) \in \mathcal{P}$, we can define the negative pair set $\bar{\mathcal{P}}(u_i, v_j)$ by replacing e_i or e_j with their neighbors (Mao et al., 2020; Zhu et al., 2021b). Then we use the following contrastive loss with negative sample pair $(u_{i'}, v_{j'}) \in \bar{\mathcal{P}}(u_i, v_j)$:

$$\sum_{i',j'} \max\{d_M(e_i^u, e_j^v) - d_M(e_{i'}^u, e_{j'}^v) + \lambda, 0\}$$

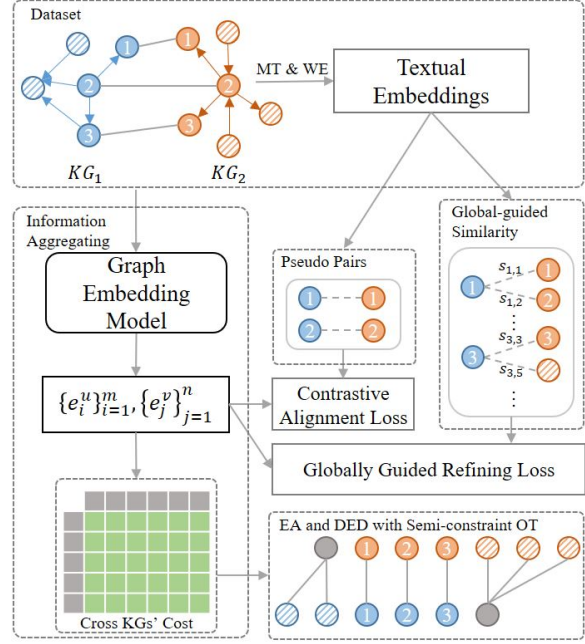


Figure 1: The Framework of SoTeard. The circles with a number are matchable entities, and the circles with slash denote dangling entities. The gray circles are the virtual entities and the gray rectangles in distance matrix denotes distance between virtual entity to other entities. MT and WE refer to machine translation and word embeddings.

where λ is the margin, and $d_M(\cdot, \cdot)$ is the Manhattan distance following previous works (Zhu et al., 2021a). The overall alignment loss \mathcal{L}_a is the summation over all pseudo pairs and their negative sample pairs.

Globally guided refining loss: The alignment loss \mathcal{L}_a only trains pseudo entity pairs and their negative samples. To make full use of entity textual information and learn embedding for all entities, we add a globally guided refining loss. We denote \mathcal{Q} as all (u_i, v_j) pairs, where v_j is one of the top N similar entities of u_i based on textual similarity $\{s_{ij}\}$, and N is a hyper-parameter. Negative sample set $\bar{\mathcal{Q}}(u_i, v_j)$ also replaces e_i or e_j with their neighbors. For each $(u_i, v_j) \in \mathcal{Q}$ and its all negative samples $(u_{i'}, v_{j'}) \in \bar{\mathcal{Q}}(u_i, v_j)$, we set:

$$s_{ij} \sum_{i',j'} \max\{d_M(e_i^u, e_j^v) - d_M(e_{i'}^u, e_{j'}^v) + \lambda, 0\}$$

Here we multiply s_{ij} to the contrastive loss, to induce the model paying more attention to the entity pairs with higher textual similarity. The overall globally guided loss \mathcal{L}_g is the summation over all entity pairs and their negative sample pairs.

The overall loss for entity embeddings is

$$\mathcal{L} = \mathcal{L}_a + w(t)\mathcal{L}_g, \quad (7)$$

where t is the training step, and $w(t)$ decreases linearly to 0 as t increases. When entity embeddings e_i^u and e_j^v are learned, the cost for our optimal transport is set as $c_{ij} = d_M(e_i^u, e_j^v)$.

For the cost for transporting entities to virtual entities, we first denote $l_i^u = \min_{1 \leq j \leq n} \{c_{ij}\}$ and $l_j^v = \min_{1 \leq i \leq m} \{c_{ij}\}$ as the smallest cost from u_i to \mathcal{G}_2 and from v_j to \mathcal{G}_1 , respectively. Next, we do grid-search of the quantiles of $\{l_i^u, 1 \leq i \leq m\}$ and $\{l_j^v, 1 \leq j \leq n\}$ in pairs as possible selection of α and β . The optimal selection of α^* and β^* achieves the best EA performance on the pseudo entity pairs set \mathcal{P} .

3.3 Integer Programming Solution

To solve the semi-constraint optimal transport in equation (6), we treat it as a mixed integer programming(MIP) as described in Section 2. Then we use a branch-and-cut algorithm to calculate the indicator solutions. The details of solution steps for equation (6) is described in Supplementary A.1.

Moreover, to further reduce the complexity of the semi-constraint optimal transport, we only consider the transports from each entity to its top- K similar entities in the target KG, noting the fact that less similar entities contain less information for alignment. This approximation also leads to more sparse sets of c_{ij} and ψ_{ij} . In Section 6.3, we show that this simplification is powerful with less computational complexity.

4 Related Work

Embedding-based Entity Alignment: The aim of embedding-based entity alignment is to encode KGs into low-dimensional vector spaces, then find nearest neighbors as the aligned entities. Recently various embedding-based EA methods have been proposed, such as TransE (Bordes et al., 2013), GCN (Kipf and Welling, 2016), GAT (Veličković et al., 2017), and their variants (Sun et al., 2017; Zhu et al., 2021b). All embedding-based EA methods adopt the information from graph structures (Chen et al., 2017), while some methods utilize textual information (Xu et al., 2019; Wu et al., 2019; Zhu et al., 2021a) or entity attributes (Sun et al., 2017; Trisedya et al., 2019).

Global Entity Alignment: Only matching entities with its nearest neighbor is a “greedy” scheme,

which is difficult to find the global optimal pair-matching for all the entities. Besides, one mismatched entity pair can disturb the greedy matching of the rest entities, and the match error can be accumulated along the greedy matching process. Therefore, global entity alignment, which considers all alignments jointly, have recently attracted considerable attention (Xu et al., 2020; Zeng et al., 2020; Zhu et al., 2021a; Lin et al., 2021). However, globally solving optimal matching costs much higher complexity. To improve the efficiency, Xu et al. (2020) decomposes the entire search space into many isolated sub-spaces and consequently restricts the cross-subspace alignment. Zeng et al. (2020) reduces the complexity by requiring the entity pairs to be stable matches and using deferred acceptance algorithm (Mullin and Stalaker, 1952; Roth, 2008) to find the alignments.

5 Experimental Setups

5.1 Datasets and Evaluation

For the entity alignment task, we follow the prior work (Sun et al., 2017; Wu et al., 2019; Zhu et al., 2021a) and test our method on the DBP15K dataset (Sun et al., 2017). For the dangling entity detection task, Sun et al. (2021) construct a DBP2.0 dataset with dangling entity labels. However, the DBP2.0 dataset does not contain textual entity name of each entity, which is incompatible for our method to extract pseudo entity pairs. Therefore, we construct a new MedED dataset to support DED task. The details are described below:

MedED Dataset Construction: The Unified Medical Language System (UMLS) (Lindberg et al., 1993) is a large-scale resource containing over 4 million unique medical concepts and over 87 million relation triples. Concepts in UMLS have several terms in different languages. We extract concepts that contain terms in the selected language as entities to construct new monolingual KG, and retain the relations between entities. For the entity names, we select the preferred terms in UMLS. The criterion of entity pairs is whether entities belong to the same concept. A dangling entity is set if its original concept is not in the other KG. We extracted the KGs of English, French, and Spanish and then constructed the KG pairs of FR-EN (French to English) and ES-EN (Spanish to English). We select 20,000 entities with the most relation triples in UMLS for the specified language, and then drop the entities unrelated to other se-

lected entities. Supplementary A.2 shows the statistics of the new dataset, MedED. For both EA and DED tasks, we split 70% of the data as the testing set. Even though our method does not rely on the training set, we keep the remaining 30% as the training set for further model comparison and ablation study.

DBP15K Dataset: DBP15K (Sun et al., 2017) contains three pairs of cross-lingual KGs, ZH-EN (Chinese to English), JA-EN (Japanese to English), and FR-EN (French to English). Each KG contains approximately 20 thousand entities, and every KG pair contains 15 thousand entity pairs (Table 6). Following the setting in previous works (Sun et al., 2017; Wu et al., 2019; Zhu et al., 2021a), we keep 70% of entity pairs for testing and 30% for training.

Evaluation Metrics: For entity alignment, we follow previous works (Xu et al., 2020; Zeng et al., 2020) and compute Hits@1 score, which indicates the percentage of the targets that have been correctly ranked in the top-1. The prior works (Sun et al., 2017, 2018; Wu et al., 2019; Zhu et al., 2021a) compute Hits@1 in a *relaxed setting* in which only the entities in testing pairs are taken into account, assuming that any source entity has a counterpart in the target KG. To the relaxed evaluation, we also compute Hits@1 in a *practical setting* in which for every testing entity, the list of candidate counterparts consists of all entities in the other KG. For dangling entity detection, we compute the classification precision, recall, and F1-score as evaluation measurements.

5.2 Baselines

For entity alignment, we compare our method with following baselines: (1) Init-Emb, the entity textual embeddings used in SoTead; (2) the supervised EA methods: MTransE (Chen et al., 2017), JAPE (Sun et al., 2017), BootEA (Sun et al., 2018), RDGCN (Wu et al., 2019), CEA (Zeng et al., 2020), RNM (Zhu et al., 2021b), RAGA (Zhu et al., 2021a), SelfKG (Liu et al., 2021), and EchoEA (Lin et al., 2021); (3) the unsupervised EA methods: SelfKG (Liu et al., 2021), UEA (Zeng et al., 2021b), and SEU (Mao et al., 2021). Here the CEA, RAGA, and EchoEA use the deferred acceptance algorithm (DAA) to globally align entities.

Our proposed method is also compatible with supervised training entity pairs, so we provide both unsupervised and supervised versions of our method: (1) the unsupervised method, SoTead, described in Section 3. (2) the supervised version of

	DBP15K			MedED	
	ZH-EN	JA-EN	FR-EN	FR-EN	SP-EN
<u>Init-Emb</u>	57.5	65.0	81.8	71.6	68.5
Supervised					
MTransE	30.8	27.9	24.4	-	-
JAPE	73.1	82.8	-	-	-
BootEA	62.9	62.2	65.3	-	-
RDGCN	70.8	76.7	88.6	-	-
<u>RNM</u>	84.0	87.2	93.8	-	-
GM-EHD-JEA	73.6	79.2	92.4	-	-
CEA	78.7	86.3	97.2	-	-
<u>RAGA</u>	87.3	90.9	96.6	96.2	97.0
<u>EchoEA</u>	89.1	93.2	98.9	-	-
<u>SoTead*</u>	91.5	94.1	98.4	97.4	97.9
Unsupervised					
SelfKG	82.9	89.0	95.9	-	-
<u>SoTead</u>	87.7	91.5	97.5	97.0	97.6
UEA(word+string)	91.3	94.0	95.3	-	-
SEU(word+char)	90.0	95.6	98.8	-	-
<u>SoTead(word+char)</u>	93.2	96.8	99.5	-	-

Table 1: The results of Hits@1 on EA task on DBP15K and MedED (relaxed setting). The underlined models use the same initial entity embeddings. The CEA, RAGA and EchoEA use the DAA for global alignment. The dashed line split the unsupervised part into model merely using word embedding and using word embedding and char-level or string-level information.

SoTead, which combines the training entity pairs and the pseudo entity pairs for the alignment loss, denoted as SoTead*.

5.3 Implementation Details

Following Wu et al. (2019), we translate entity names in MedED to English via Google Translate and then use mean of word vector from GloVe (Pennington et al., 2014) to obtain textual entity embeddings. For entities in DBP15K, we inherit the initial embeddings used in previous works (Wu et al., 2019; Zeng et al., 2021b; Zhu et al., 2021a,b; Lin et al., 2021). The threshold for pseudo pairs ε is 0.99, and $N = 3$ in globally guided refining loss. The initial value of $w(t)$ is 0.3 and $w(t)$ decreases linearly to 0 at 1/4 of the total training steps. We follow GNN setups from RAGA (Zhu et al., 2021a) to encode the enhanced entity embeddings. The default value of K is set to 100. We grid search 100 paired quantiles of $\{I_i^u, 1 \leq i \leq m\}$ and $\{I_j^v, 1 \leq j \leq n\}$ with $K = 10$ to obtain α^* and β^* .

6 Experimental Results

6.1 Entity Alignment Results

Table 1 shows the results of EA on DBP15K and MedED datasets. Following the previous work, we adopt the relaxed evaluation setting. The results

	FR-EN				ES-EN			
	EA		DED		EA		DED	
	H@1	P	R	F	H@1	P	R	F
RAGA	78.7	-	-	-	82.7	-	-	-
SoTead(DAA)	77.4	-	-	-	87.0	-	-	-
Distance	-	78.1	73.4	75.7	-	78.6	86.1	82.2
SoTead								
K=1	79.8	96.1	79.4	86.9	86.0	90.4	84.2	87.2
K=10	80.3	96.3	75.3	84.5	87.4	93.5	68.4	79.0
K=100	80.5	96.4	74.8	84.2	87.7	93.3	64.6	76.4
SoTead*	82.6	97.6	65.4	78.3	90.1	94.1	69.4	79.9

Table 2: EA and DED results on MedED (practical setting). $\widehat{H@1}$, P, R, and F denotes Hits@1, precision, recall, and F-score. $K = 1, 10, 100$ refers to the proposed global alignment method that keeps the top K ($= 1, 10, 100$) rank similarity entities for each entity. The SoTead(DAA) and RAGA use the DAA for global alignment.

with practical evaluation settings for Hits@1 are listed in the Supplementary A.3.

When compared under **supervised** setups, the SoTead achieves comparable results on DBP15K. Without supervision, the SoTead outperforms all competing methods except the EchoEA method. Besides, the gap between SoTead and EchoEA is marginal. In addition, SoTead* outperforms all methods in MedED. When compared under **unsupervised** setups, SoTead outperforms all other unsupervised baselines. Besides, UEA and SEU use the extra string-level and char-level information from entity names respectively to enhance the models, denoted as UEA(word+string) and SEU(word+char). For fair comparison, we follow SEU and add the char-level distance to the cost between entities cross KGs. The the char-level distance is the Manhattan distance between bi-gram vectors from translated entity names used in SEU. This model is denoted as SoTead(word+char) and is superior to UEA and SEU.

6.2 Dangling Entity Detection Results

Table 2 shows the results of EA and DED on MedED. Note that global alignment with DED should consider all entities. We select the practical setting in the EA evaluation.

As shown in Table 2, for the EA task, SoTead achieves better results compared to the supervised RAGA and the variants of our method with DAA. For the DED task, our method focuses more on the precision in recognizing dangling entities. The results of SoTead and SoTead* are also much better than the Distance, which is the same as the

	DBP15K			MedED	
	ZH	JA	FR	FR	ES
SoTead	87.7	91.5	97.5	97.0	97.6
w/o OT	77.9	82.0	92.1	89.5	89.3
w/o dec.	87.3	91.0	97.3	96.9	97.3
w/o \mathcal{L}_g	87.5	91.0	97.3	97.1	97.5
SoTead(DAA)	84.7	89.1	96.2	95.5	95.6

Table 3: Hits@1 results of method variants (relaxed setting) in the EA task. The OT refers to the semi-constraint optimal transport module. The dec. is the weight decreasing mechanism of the globally guided loss, \mathcal{L}_g . ZH, JA, FR and ES denotes the KG pairs ZH-EN, JA-EN, FR-EN and ES-EN.

threshold-based unsupervised attempt of Zhao et al. (2020) on DED by searching the best threshold on the dangling training set. These results indicate that SoTead successfully uses unsupervised EA to enhance DED, since DED with high precision reduces the scope of EA and enhances the performance.

6.3 Empirical Runtime Analysis

Choosing an appropriate K can effectively reduce the time complexity of the semi-constraint OT, since the solving process of the semi-constraint OT could be finished in less than 7, 60, and 5,00 seconds for $K = 1, 10, 100$ in MedED. Furthermore, the results with different K in Table 2 show that the performance of $K = 10$ and $K = 100$ is similar, implying that much larger value of K may not bring significant improvement and $K = 100$ is enough for the proposed method considering the time consuming.

6.4 Ablation Study

In Table 3, we test variants by removing the weight decreasing mechanism of the globally guided refining loss \mathcal{L}_g and the \mathcal{L}_g from SoTead. Besides, in Table 3, we replace the proposed semi-constraint OT with DAA. Table 4 provides other variants in practical setting. Our main observations are:

1. The semi-constraint OT is stable and effective, causing significant improvements (4.6~9.8 Hits@1) compared with the SoTead without semi-constraint OT (Table 3).

2. Ablating the globally guided refining similarity \mathcal{L}_g and the weight decreasing mechanism of \mathcal{L}_g leads to a decrease in most cases (Table 3), indicating they are usually helpful.

3. Introducing the virtual entity is necessary. In Table 4, the SoTead without virtual entity gains a remarkable decrease on EA from 80.3 to 55.5 in FR-EN and from 87.4 to 65.2 in ES-EN, and cannot

	FR-EN		ES-EN	
	EA	DED	EA	DED
SoTead	80.3	84.5	87.4	79.0
w/o virtual	55.5	-	65.2	-
w. golden α, β	80.9	80.3	87.4	79.0
SoTead(CODER)	88.4	86.3	93.3	86.5

Table 4: Results of method variants (practical setting) in MedED. We report Hits@1 and F-score for EA and DED. The w/o virtual denotes the semi-constraint OT without the virtual entities. The w. golden α, β denote that the α and β in the semi-constraint OT are selected by the EA training set. SoTead(CODER) replaces Glove embeddings with a medical language model.

	ZH-EN	JA-EN	FR-EN
Glove(initial)	57.0	63.3	80.7
Glove(SoTead)	84.7	89.0	96.6
word2vec(initial)	44.6	49.6	59.4
word2vec(SoTead)	65.0	70.6	79.6
FastText(initial)	49.7	54.3	64.3
FastText(SoTead)	74.7	77.3	88.1
MUSE(initial)	57.9	61.1	76.6
MUSE(SoTead)	83.3	87.0	95.8

Table 5: The EA results of Hits@1 on DBP15K for SoTead trained with different resources of embeddings. ‘‘initial’’ denotes the entity embeddings initialized by taking the mean of word embeddings.

be applied to the DAD task.

4. Figure 2 shows that the proposed method for searching proper α^* and β^* almost reaches the best Hits@1. Similar conclusion is shown in Table 4 with the marginal difference between the result of α^* and β^* and the golden selection of α and β based on the EA training entity pairs.

5. The proportion of how many pseudo entity pairs can play an equal role as true entity pairs changes depending on the KG pairs in Figure 3, but it is still valid to obtain pseudo entity pairs when true entity pairs are unavailable since the proportion is not very low.

To further understand the influence of the quality of initial embeddings, we replace the GloVe in MedED with a pretrained medical language model (LM), the English version of CODER (Yuan et al., 2020), and show that a proper domain-specific LM trained on a large KG can bring better results (in Table 4). Moreover, we test the effect of different initial word embedding on SoTead performance. We use Glove, word2vec, FastText, and MUSE (in Table 5). The MUSE is a multilingual word embeddings method, and we generate the initial entity embeddings directly without machine translation. Table 5 indicates that the performance of SoTead re-

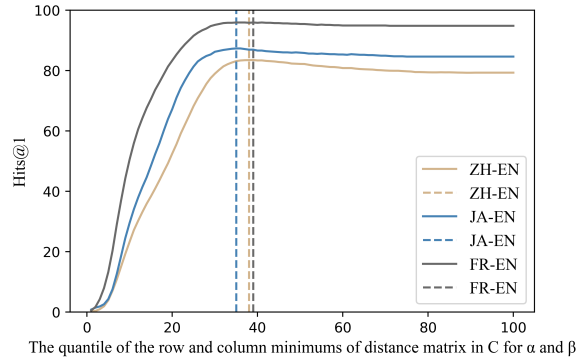


Figure 2: The Hits@1 in DBP15K (practical setting) for the SoTead according to different value selection of the α and β . The solid line denotes the result of SoTead and dashed line in corresponding color denotes α^* and β^* selected by the proposed selection strategy.

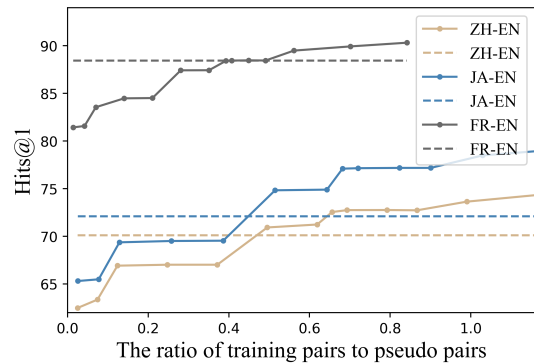


Figure 3: The Hits@1 in DBP15K (practical setting) for the SoTead without \mathcal{L}_g and semi-constraint OT. The solid line and dashed line denotes the method trained with the training entity pairs and pseudo entity pairs, respectively.

lies on the quality of the textual information, since the Hits@1 of SoTead highly related to the Hits@1 of the initial embeddings.

7 Conclusion

We propose a novel unsupervised method, SoTead, for entity alignment and dangling entity detection via a semi-constraint optimal transport. By introducing virtual entities on KGs, our method relaxes the alignment constraints, and jointly detects the dangling entities and matchable entity pairs. In experiments, our method reaches state-of-the-art performance and supports the point that dangling entity detection enhances the entity alignment models. Besides, we build a new cross-lingual medical knowledge graph dataset, MedED, which supports both entity alignment and dangling entity detection tasks. We hope this work provide insight for real-world knowledge graph processing.

References

- David Alvarez-Melis and Tommi S Jaakkola. 2018. Gromov-wasserstein alignment of word embedding spaces. *arXiv preprint arXiv:1809.00013*.
- Egon Balas, Sebastián Ceria, and Gérard Cornuéjols. 1993. A lift-and-project cutting plane algorithm for mixed 0–1 programs. *Mathematical programming*, 58(1):295–324.
- Antoine Bordes, Nicolas Usunier, Alberto Garcia-Duran, Jason Weston, and Oksana Yakhnenko. 2013. Translating embeddings for modeling multi-relational data. *Advances in neural information processing systems*, 26.
- Yixin Cao, Xiang Wang, Xiangnan He, Zikun Hu, and Tat-Seng Chua. 2019. Unifying knowledge graph learning and recommendation: Towards a better understanding of user preferences. In *The world wide web conference*, pages 151–161.
- Liqun Chen, Shuyang Dai, Chenyang Tao, Dinghan Shen, Zhe Gan, Haichao Zhang, Yizhe Zhang, and Lawrence Carin. 2018. Adversarial text generation via feature-mover’s distance. *arXiv preprint arXiv:1809.06297*.
- Liqun Chen, Yizhe Zhang, Ruiyi Zhang, Chenyang Tao, Zhe Gan, Haichao Zhang, Bai Li, Dinghan Shen, Changyou Chen, and Lawrence Carin. 2019. Improving sequence-to-sequence learning via optimal transport. *arXiv preprint arXiv:1901.06283*.
- Muhao Chen, Yingtao Tian, Mohan Yang, and Carlo Zaniolo. 2017. Multilingual knowledge graph embeddings for cross-lingual knowledge alignment. In *Proceedings of the 26th International Joint Conference on Artificial Intelligence*, pages 1511–1517.
- George Dantzig. 2016. *Linear programming and extensions*. Princeton university press.
- George B Dantzig, Alex Orden, Philip Wolfe, et al. 1955. The generalized simplex method for minimizing a linear form under linear inequality restraints. *Pacific Journal of Mathematics*, 5(2):183–195.
- Luis Galárraga, Simon Razniewski, Antoine Amarilli, and Fabian M Suchanek. 2017. Predicting completeness in knowledge bases. In *Proceedings of the tenth acm international conference on web search and data mining*, pages 375–383.
- Saul I Gass. 2003. *Linear programming: methods and applications*. Courier Corporation.
- Qiao Jin, Zheng Yuan, Guangzhi Xiong, Qianlan Yu, Chuanqi Tan, Mosha Chen, Songfang Huang, Xiaozhong Liu, and Sheng Yu. 2021. Biomedical question answering: A comprehensive review. *arXiv preprint arXiv:2102.05281*.
- Thomas N Kipf and Max Welling. 2016. Semi-supervised classification with graph convolutional networks. *arXiv preprint arXiv:1609.02907*.
- Matt Kusner, Yu Sun, Nicholas Kolkin, and Kilian Weinberger. 2015. From word embeddings to document distances. In *International conference on machine learning*, pages 957–966. PMLR.
- Xueyuan Lin, Wenyu Song, Haoran Luo, et al. 2021. Echoea: Echo information between entities and relations for entity alignment. *arXiv preprint arXiv:2107.03054*.
- Donald AB Lindberg, Betsy L Humphreys, and Alexa T McCray. 1993. The unified medical language system. *Yearbook of Medical Informatics*, 2(01):41–51.
- Xiao Liu, Haoyun Hong, Xinghao Wang, Zeyi Chen, Evgeny Kharlamov, Yuxiao Dong, and Jie Tang. 2021. A self-supervised method for entity alignment. *arXiv preprint arXiv:2106.09395*.
- Xin Mao, Wenting Wang, Huimin Xu, Yuanbin Wu, and Man Lan. 2020. Relational reflection entity alignment. In *Proceedings of the 29th ACM International Conference on Information & Knowledge Management*, pages 1095–1104.
- Xinnian Mao, Wenting Wang, Yuanbin Wu, and Man Lan. 2021. From alignment to assignment: Frustratingly simple unsupervised entity alignment. In *Proceedings of the 2021 Conference on Empirical Methods in Natural Language Processing*, pages 2843–2853.
- John E Mitchell. 2002. Branch-and-cut algorithms for combinatorial optimization problems. *Handbook of applied optimization*, 1:65–77.
- FJ Mullin and John M Stalnak. 1952. The matching plan for internship placement. *J. MED. EDUC.*, 27:193–193.
- Manfred Padberg and Giovanni Rinaldi. 1991. A branch-and-cut algorithm for the resolution of large-scale symmetric traveling salesman problems. *SIAM review*, 33(1):60–100.
- Heiko Paulheim. 2018. How much is a triple? estimating the cost of knowledge graph creation.
- Jeffrey Pennington, Richard Socher, and Christopher D Manning. 2014. Glove: Global vectors for word representation. In *Proceedings of the 2014 conference on empirical methods in natural language processing (EMNLP)*, pages 1532–1543.
- Alvin E Roth. 2008. Deferred acceptance algorithms: History, theory, practice, and open questions. *International Journal of game Theory*, 36(3):537–569.
- Tim Salimans, Han Zhang, Alec Radford, and Dimitris Metaxas. 2018. Improving gans using optimal transport. *arXiv preprint arXiv:1803.05573*.
- Denis Savenkov and Eugene Agichtein. 2016. Crqa: Crowd-powered real-time automatic question answering system. In *Fourth AAAI conference on human computation and crowdsourcing*.

- Zequn Sun, Muhao Chen, and Wei Hu. 2021. Knowing the no-match: Entity alignment with dangling cases.
- Zequn Sun, Wei Hu, and Chengkai Li. 2017. Cross-lingual entity alignment via joint attribute-preserving embedding. In *International Semantic Web Conference*, pages 628–644. Springer.
- Zequn Sun, Wei Hu, Qingheng Zhang, and Yuzhong Qu. 2018. Bootstrapping entity alignment with knowledge graph embedding. In *Proceedings of the 27th International Joint Conference on Artificial Intelligence*, pages 4396–4402.
- Bayu Distiawan Trisedya, Jianzhong Qi, and Rui Zhang. 2019. Entity alignment between knowledge graphs using attribute embeddings. In *Proceedings of the AAAI Conference on Artificial Intelligence*, volume 33, pages 297–304.
- Petar Veličković, Guillem Cucurull, Arantxa Casanova, Adriana Romero, Pietro Lio, and Yoshua Bengio. 2017. Graph attention networks. *arXiv preprint arXiv:1710.10903*.
- Cédric Villani. 2009. *Optimal transport: old and new*, volume 338. Springer.
- Zhichun Wang, Qingsong Lv, Xiaohan Lan, and Yu Zhang. 2018. Cross-lingual knowledge graph alignment via graph convolutional networks. In *Proceedings of the 2018 Conference on Empirical Methods in Natural Language Processing*, pages 349–357.
- Laurence A Wolsey and George L Nemhauser. 1999. *Integer and combinatorial optimization*, volume 55. John Wiley & Sons.
- Yuting Wu, Xiao Liu, Yansong Feng, Zheng Wang, Rui Yan, and Dongyan Zhao. 2019. Relation-aware entity alignment for heterogeneous knowledge graphs. *arXiv preprint arXiv:1908.08210*.
- Chenyan Xiong, Russell Power, and Jamie Callan. 2017. Explicit semantic ranking for academic search via knowledge graph embedding. In *Proceedings of the 26th international conference on world wide web*, pages 1271–1279.
- Kun Xu, Linfeng Song, Yansong Feng, Yan Song, and Dong Yu. 2020. Coordinated reasoning for cross-lingual knowledge graph alignment. In *Proceedings of the AAAI Conference on Artificial Intelligence*, volume 34, pages 9354–9361.
- Kun Xu, Liwei Wang, Mo Yu, Yansong Feng, Yan Song, Zhiguo Wang, and Dong Yu. 2019. Cross-lingual knowledge graph alignment via graph matching neural network. In *Proceedings of the 57th Annual Meeting of the Association for Computational Linguistics*, pages 3156–3161.
- Mo Yu, Wenpeng Yin, Kazi Saidul Hasan, Cicero dos Santos, Bing Xiang, and Bowen Zhou. 2017. Improved neural relation detection for knowledge base question answering. In *Proceedings of the 55th Annual Meeting of the Association for Computational Linguistics (Volume 1: Long Papers)*, pages 571–581.
- Zheng Yuan, Zhengyun Zhao, Haixia Sun, Jiao Li, Fei Wang, and Sheng Yu. 2020. Coder: Knowledge infused cross-lingual medical term embedding for term normalization. *arXiv preprint arXiv:2011.02947*.
- Kaisheng Zeng, Chengjiang Li, Lei Hou, Juanzi Li, and Ling Feng. 2021a. A comprehensive survey of entity alignment for knowledge graphs. *AI Open*, 2:1–13.
- Weixin Zeng, Xiang Zhao, Jiuyang Tang, Xinyi Li, Minnan Luo, and Qinghua Zheng. 2021b. Towards entity alignment in the open world: An unsupervised approach. *arXiv preprint arXiv:2101.10535*.
- Weixin Zeng, Xiang Zhao, Jiuyang Tang, and Xuemin Lin. 2020. Collective entity alignment via adaptive features. In *2020 IEEE 36th International Conference on Data Engineering (ICDE)*, pages 1870–1873. IEEE.
- Ziheng Zhang, Hualuo Liu, Jiaoyan Chen, Xi Chen, Bo Liu, YueJia Xiang, and Yefeng Zheng. 2020. An industry evaluation of embedding-based entity alignment. In *Proceedings of the 28th International Conference on Computational Linguistics: Industry Track*, pages 179–189.
- Xiang Zhao. 2020. Towards knowledge graphs federations: Issues and technologies. In *Asia-Pacific Web (APWeb) and Web-Age Information Management (WAIM) Joint International Conference on Web and Big Data*, pages 66–79. Springer.
- Xiang Zhao, Weixin Zeng, Jiuyang Tang, Wei Wang, and Fabian Suchanek. 2020. An experimental study of state-of-the-art entity alignment approaches. *IEEE Transactions on Knowledge & Data Engineering*, (01):1–1.
- Renbo Zhu, Meng Ma, and Ping Wang. 2021a. Raga: Relation-aware graph attention networks for global entity alignment. In *PAKDD (1)*, pages 501–513. Springer.
- Yao Zhu, Hongzhi Liu, Zhonghai Wu, and Yingpeng Du. 2021b. Relation-aware neighborhood matching model for entity alignment. In *Proceedings of the AAAI Conference on Artificial Intelligence*, volume 35, pages 4749–4756.

A Supplementary

A.1 Branch-and-Cut Algorithm

We describe the branch-and-cut algorithm (Mitchell, 2002) to solve the proposed semi-constraint optimal transport (SOP) as follows:

Algorithm 1 Branch-and-Cut Algorithm

- 1: **Step 1.** Initialization: Denote the initial SOP as SOP^0 and the active nodes $L = \{SOP^0\}$. Set the upper bound of the object function $z = \sum_{i=1}^m \sum_{j=1}^n c_{ij} \psi_{ij} + \sum_{i=1}^m c_{i0} \psi_{i0} + \sum_{j=1}^n c_{0j} \psi_{0j}$ to be $\bar{z} = +\infty$ and set the lower bound of problem $l \in L$ to be $z_l = -\infty$.
 - 2: **Step 2.** Termination: If $L = \emptyset$, then the solution ψ^* which yielded the incumbent objective value \bar{z} is optimal. If no such ψ^* exists, the SOP is infeasible.
 - 3: **Step 3** Problem selection: Select and delete a problem SOP^l from L .
 - 4: **Step 4.** Relaxation: Solve the linear programming relaxation of SOP^l . If the relaxation is infeasible, set $z^l = +\infty$ and go to Step 6. Let z^l denote the optimal objective value of the relaxation if it is finite and let ψ^{lR} be an optimal solution; otherwise set $z^l = -\infty$.
 - 5: **Step 5.** Add cutting planes: If desired, search for cutting planes that are violated by ψ^{lR} ; if any are found, add them to the relaxation and return to Step 4.
 - 6: **Step 6.** Fathoming and Pruning:
 - 7: (a) If $z^l \geq \bar{z}$, go to Step 2.
 - 8: (b) If $z^l < \bar{z}$ and ψ^{lR} is integral feasible, update $\bar{z} = z^l$ and delete all $l \in L$ with $z_l \geq \bar{z}$. Go to Step 2.
 - 9: **Step 7** Partitioning: Let $\{S^{lj}\}_{j=1}^{j=k}$ be a partition of the constraint set S^l of SOP^l . Add $\{SOP^{lj}\}_{j=1}^{j=k}$ to L , where SOP^{lj} is SOP^l with feasible region restricted to S^{lj} and z_{lj} for $j = 1, \dots, k$ is set to the value of z^l for the parent problem l . Go to Step 2.
-

A.2 Data Statistics

We provide the statistics of MedED and DBP15K in Table 6, including entities, types of relations, relations triples, entity pairs, and dangling entities in each KG.

Datasets	#Ent.	#Rel.	#Trip.	#Pairs	#Dang.	
MedED	FR	19,382	431	455,368	6,365	13,017
	EN	18,632	622	841,792	6,365	12,267
MedED	ES	19,228	546	594,130	11,153	8,075
	EN	18,632	622	841,792	11,153	7,479
DBP15K	ZH	19,388	1,700	70,414	15,000	-
	EN	19,572	1,322	95,142	15,000	-
DBP15K	JA	19,814	1,298	77,214	15,000	-
	EN	19,780	1,152	93,484	15,000	-
DBP15K	FR	19,661	902	105,998	15,000	-
	EN	19,993	1,207	115,722	15,000	-

Table 6: Statistics of MedED and DBP15K.

A.3 Practical Evaluation Results

For completeness, this supplementary reports the EA results on DBP15K in practical evaluation setting (Table 7). We compared our methods with the RAGA, since we adopt the part of graph embedding in RAGA in our framework.

	ZH-EN		JA-EN		FR-EN	
	$\hat{\text{@}}1$	$\hat{\text{@}}10\text{MRR}$	$\hat{\text{@}}1$	$\hat{\text{@}}10\text{MRR}$	$\hat{\text{@}}1$	$\hat{\text{@}}10\text{MRR}$
Init-Emb	57.068.6	61.1	63.375.3	67.6	80.789.0	83.5
RAGA(w/o DAA)	72.590.3	79.0	77.393.1	82.9	88.497.2	91.7
SoTead(w/o OT)	75.189.2	80.2	79.391.8	83.9	91.197.4	93.4
RAGA	83.4		74.2		92.9	
SoTead(DAA)	79.9		76.9		93.5	
SoTead	84.7		89.0		96.6	

Table 7: EA results on DBP15K (practical setting). $\hat{\text{@}}1$ and $\hat{\text{@}}10$ denotes the Hits@1 and Hits@10. In the part of local alignment, RAGA(w/o DAA) and SoTead(w/o OT) refer to the RAGA without DAA and SoTead without OT. The SoTead(DAA) refers to the variant of SoTead by replacing the semi-constraint OT with DAA. MRR is the average of the reciprocal of the rank results.